Calculating carbon nanotube–catalyst adhesion strengths

Peter Larsson,[1] J. Andreas Larsson,[2] Rajeev Ahuja,[1] Feng Ding,[3,4] Boris I. Yakobson,[4] Haiming Duan,[3,*] Arne Rosén,[3] and Kim Bolton[3,5]

[1]*Condensed Matter Theory Group, Department of Physics, Uppsala University, P.O. Box 530, SE-751 21 Uppsala, Sweden*

[2]*Tyndall National Institute, University College Cork, Lee Maltings, Prospect Row, Cork, Ireland*

[3]*Physics Department, Göteborg University, Göteborg, SE-412 96, Sweden*

[4]*ME&MS Department, Rice University, Houston, Texas 77005, USA*

[5]*School of Engineering, University College of Borås, Borås SE-501 90, Sweden*

(Received 7 November 2006; published 20 March 2007)

Density-functional theory is used to assess the validity of modeling metal clusters as single atoms or rings of atoms when determining adhesion strengths between clusters and single-walled carbon nanotubes (SWNTs). Representing a cluster by a single atom or ring gives the correct trends in SWNT-cluster adhesion strengths (Fe≈Co>Ni), but the single-atom model yields incorrect minimum-energy structures for all three metals. We have found that this is because of directional bonding between the SWNT end and the metal cluster, which is captured in the ring model but not by the single atom. Hence, pairwise potential models that do not describe directional bonding correctly, and which are commonly used to study these systems, are expected to give incorrect minimum-energy structures.

DOI: 10.1103/PhysRevB.75.115419 PACS number(s): 68.43.Bc, 68.43.Fg, 73.22.−f, 73.63.Fg

INTRODUCTION

Since their discovery in 1993,[1,2] there has been an immense amount of research into the growth and applications of single-walled carbon nanotubes (SWNTs). One of the most challenging applications is in electronics,[3] where both the metallic and semiconducting properties of the SWNTs are exploited. For this to be realized, one needs to separate or selectively grow SWNTs based on their electronic properties. Although significant advances have been made in this area,[4–8] there are still no efficient methods for SWNT separation, and all production methods yield a mixture of metallic and semiconducting nanotubes.

Computational methods complement experiment by deepening our understanding of the SWNT growth mechanism, and hence can help to identify ways to control the metallicity through the chirality of the SWNTs. Computations have an advantage over experiment in that they allow complete control, manipulation, and monitoring of the atomic positions, but they often require approximations. For example, molecular-dynamics methods rely on the validity of the force fields,[9,10] and density-functional theory (DFT) methods—where the interatomic forces are handled accurately—are often based on static, zero Kelvin structures or very short dynamic simulations of small systems.[11–15] One therefore needs to be aware of these approximations and the effect that they may have on the relevance of the results, since SWNTs are usually produced at high temperatures and with added complexity (e.g., inclusion of carbon feedstock, alloyed catalysts with defects, and interactions with the surface for supported catalysts).[16]

It is known that the size of the computational model may affect the results. For example, previous work has shown that electronic properties of short SWNTs depend on the nanotube length,[17] and hence sufficiently long nanotubes need to be used in the calculations. In this work, we focus on the adhesion between SWNTs and metal clusters. These systems are relevant to SWNT growth since sufficiently strong adhesion is necessary to maintain an open end—and hence the continued growth—of SWNTs.[10,18] Our studies show that metals that are commonly used to catalyze SWNT growth, Fe, Co, and Ni, have large adhesion energies, and subsequently, these metals are the focus of the present work. In particular, we investigate the effect of the SWNT length and what model is used for the catalyst metal nanoparticle—whether it is represented as a complete stable cluster, a ring, or as a single atom—on the adhesion energy and structure of the SWNT-metal cluster complex. In addition to the lower computational costs, the motivation to model the cluster as an atom or ring is that previous studies related to SWNT growth have used the former model,[13] whereas we propose the latter model as a simplification compared to the use of full clusters, since the ring model allows for all SWNT dangling bonds to be bonded to metal atoms, as is the case with the cluster. In addition to the size of the model affecting the results, we have also checked that different density functionals, one-electron basis, and other model parameters do not lead to conflicting conclusions.

METHOD

The Vienna *ab initio* simulation program[19–21] (VASP) has been used in this work. Calculations were performed with the PW91 (Ref. 22) functional and an ultrasoft pseudopotential with a plane-wave cutoff of 290 eV for the single metal atom and ring models and the projector augmented wave method with a plane-wave cutoff of 400 eV for the metal clusters. Spin-polarized and nonpolarized calculations yield very similar adhesion energies, which are important since the cluster, which is magnetic at 0 K (Refs. 23 and 24), is molten and hence nonmagnetic under typical growth conditions.[25] We have also obtained similar trends in preliminary calculations with TURBOMOLE (Ref. 26) using atom-centered Gaussian basis sets and the Perdew-Burke-Ernzerhof[27] (PBE) func-

tional, showing that the choice of basis set and functional does not significantly affect the results. These results will appear in a future publication.

This work focuses on the (5,0) SWNT-M_{13} system, where M is either Ni, Co, or Fe. We also present results for the (10,0) SWNT and (5,5) SWNT-M_{55} systems to put these results in perspective. The diameters of the clusters are similar to those of the SWNTs, which is often observed experimentally[28,29] and has been shown by molecular-dynamics simulations[30,31] to successfully grow nanotubes. The total number of dangling bonds of an (n,m) SWNT is $n+m$ at either end. In the present calculations, these bonds are passivated by hydrogen atoms at the passive end and the metal cluster at the growing end. The adhesion energy, which is the energy difference between the geometry-optimized SWNT-cluster system and the separated SWNT and cluster systems, is given in eV/atom, where the number of atoms is $n+m$. Although the energy of the separated metal cluster is obtained at its optimized geometry, the structure of the isolated SWNT is not completely reoptimized since this results in partial closure of the unpassivated end for thin nanotubes [e.g, (5,0) SWNTs]. This does not occur for larger diameter nanotubes [e.g., (5,5) and (10,0) SWNTs] that represent more stable and thus naturally abundant nanotubes, and to facilitate comparison between small and large diameter SWNTs, results when the SWNT are not reoptimized are shown. In fact, as is shown in the Results and Discussion section, the adhesion energies that were obtained when reoptimizing the isolated SWNTs show the same trends, but different absolute values.

The adhesion energy is also calculated when modeling the cluster as a ring, where the ring consists of $n+m$ metal atoms. In some cases it was necessary to constrain the metal ring geometry so that a smaller cluster, which might penetrate the nanotube and not be a representative model of the larger cluster, is not formed during optimization. This constraint, where the ring has the same diameter as the SWNT, is used to compare the results with the full cluster calculations and so tries to mimic the atoms of the cluster that are directly bonded to the nanotube open end. For comparison, we report calculations that allow total relaxation of all atoms, but this, in some cases, gives contracting rings which cannot be used to accurately estimate adhesion energies. In addition, the energy of the separated metal ring is obtained at the same geometry as when it was attached to the SWNT, since reoptimization results in the formation of an M_{n+m} metal cluster which is not representative of the M_{13} (or M_{55}) cluster that is being modeled.

The adhesion strength of a single metal atom to the SWNT was obtained in a similar manner, with the atom being constrained to be on the same cylindrical plane as the C atoms of the SWNT wall. Similar to previous calculations,[13] the dangling carbon bonds that are not attached to the metal atom are left unpassivated. The energy units are eV/atom, where the number of atoms is 1.

RESULTS AND DISCUSSION

Our calculations show that modeling a (5,0) SWNT of different lengths does not significantly change the adhesion energy. For example, the adhesion energies between the SWNT and the constrained five-atom Ni ring (obtained from VASP) using 20, 30, and 40 carbon atom nanotubes are −2.70, −2.79, and −2.82 eV/atom, respectively. These energies are obtained when the metal ring atoms are in the top sites described below (i.e., each metal atom lies on top of one end carbon atom). Hence, all results presented below are for (5,0) SWNTs containing 30 carbon atoms. We have used (10,0) and (5,5) SWNTs of comparable length that contain 60 carbon atoms.

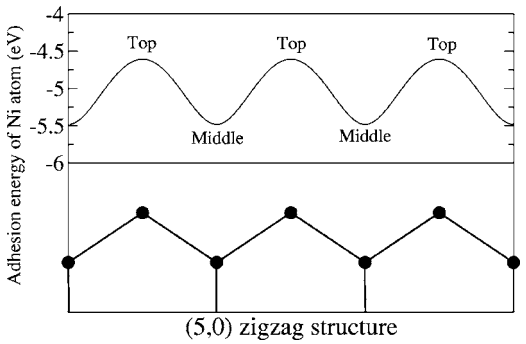

FIG. 1. Adhesion energy of a single Ni atom bonded to different sites at the end of a (5,0) SWNT.

Figure 1 shows the adhesion energy of a single Ni atom that is bonded to different sites at the end of the (5,0) SWNT. The SWNT has been projected onto the plane of the page to clarify the position of the atom above the nanotube end. The most stable structure is where the Ni atom lies in the middle of two end carbon atoms, and it is shown in Fig. 2(a). This Ni site is termed the "middle site." It should be noted (Fig. 1) that the structure with the Ni atom directly above an end carbon atom, i.e., in the "top site," is not stable. The stronger adhesion when the Ni atom occupies a middle site is because it chemically binds to two carbon atoms, and thus passivates two carbon dangling bonds.

Table I lists the adhesion energies and metal-SWNT distances for Ni, Co, and Fe when the metal atom is in the top and middle sites. The average atom-nanotube separation is the average distance between the metal atom(s) and its (their) nearest carbon atom(s). Values in parentheses are the average distances between the cluster and/or ring atoms (or the single

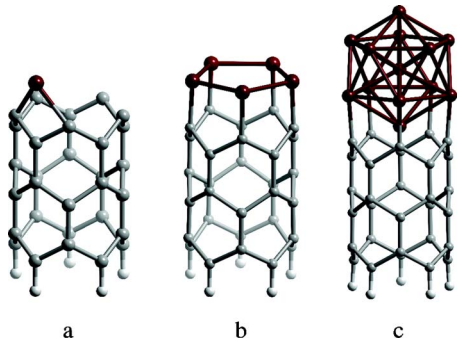

FIG. 2. (Color online) Minimum-energy structures of a (5,0) SWNT bonded to (a) a Ni atom, (b) a Ni_5 ring, and (c) a Ni_{13} cluster. The Ni atom (a) and ring (b) are constrained to the cylindrical plane of the SWNT wall.

TABLE I. Adhesion energies (eV/atom) and metal-carbon distances (Å) for Ni, Co, and Fe M_{13} cluster-(5,0) SWNT complexes as obtained by VASP (see Method section). "Atom" and "ring" refer to approximative models for M_{13} (left column). Results for completely relaxed ring structures and when the rings are constrained are shown. Energies when relaxing the isolated SWNTs (see Method section) are shown in parentheses.

		Adhesion energies (eV/atom)			Average atom-nanotube separation (Å)		
		Fe	Co	Ni	Fe	Co	Ni
Atom	Top	−5.52	−5.16	−4.61	1.76 (3.39)	1.71 (3.37)	1.76 (3.40)
	Middle	−6.93	−6.33	−5.48	1.86 (3.18)	1.87 (3.19)	1.89 (3.20)
Ring (relaxed)	Top	−3.37 (−2.80)	−3.23 (−2.68)	−2.88 (−2.34)	1.85 (3.38)	1.81 (3.42)	1.82 (3.47)
	Middle	−2.69 (−2.10)	−2.77 (−2.21)	−2.72 (−2.17)	2.02 (3.27)	1.97 (3.28)	1.97 (3.31)
Ring (constrained)	Top	−3.39	−3.20	−2.79	1.82 (3.44)	1.79 (3.42)	1.82 (3.44)
	Middle	−2.76	−2.68	−2.58	1.97 (3.26)	1.97 (3.26)	1.99 (3.28)
Cluster	Top	−2.92	−3.02	−2.86	1.97 (3.43)	1.95 (3.43)	1.92 (3.39)
	Middle	−2.61	−2.62	−2.41	2.14 (3.26)	2.16 (3.25)	2.16 (3.26)

atom) and the SWNT end atoms (for the M_{13} cluster, this is the average distance between the SWNT end atoms and the five metal atoms that are nearest to the SWNT end). For the case where the cluster is modeled as a single atom, the middle site, where two carbon dangling bonds are passivated, is the most stable position for all three metals. In addition, the Fe and Co adhesion strengths are similar and both are larger than the Ni-SWNT value.

In contrast to the single Ni atom system, the lowest-energy structure for the Ni_5 ring-SWNT structure is when the Ni atoms are in the top sites. As shown in Table I, this is valid for all metals, even when the ring coordinates are fully relaxed. In fact, the fully relaxed structures are very similar to the constrained geometries for the (5,0) SWNT complexes. Moreover, the top binding is also the preferred position for the M_{13} clusters. This reflects that when all carbon dangling bonds are passivated, other effects are prominent in determining the equilibrium structures. The minimum-energy structures for the (5,0) SWNT bound to the Ni ring and cluster are shown in Figs. 2(b) and 2(c), respectively.

As mentioned in the Method section, the adhesion energies are obtained from the constrained isolated SWNT structure. This was done since repotimizing this structure leads to contraction at the passivated SWNT end for thin SWNTs, and hence these energies cannot be directly compared with SWNTs of larger diameter which do not show this contraction. However, for completeness, we show the adhesion energies obtained when the isolated SWNT structure is not constrained during optimization, and these are shown in parentheses in Table I. It is clear from this table, and Tables II and III, that fully relaxing the isolated SWNT structure changes the magnitude of the adhesion energies but not the trends (i.e., Fe and Co adhesion strengths are similar and both are larger than the Ni-SWNT).

Although the binding sites are not correct when modeling the cluster as an atom, the trends in adhesion energy are correct. As can be seen in Table I, the (5,0) SWNT adhesion strength to Fe and Co is similar in energy and both are more strongly bound than Ni. The absolute energies are larger when modeling the clusters as single metal atoms. This is explained by the fact that two C—M bonds are formed in the middle site. To compare them to the M_{13} results, one should divide the atom adhesion strengths by 2. This is also true in a sense for the top position where C=M double bonds are formed, which is expected to amount to almost twice the binding energy of the C—M bonds in the (5,0)-M_{13} complex.

The similarity of the Fe and Co adhesion energies to SWNT ends, and the fact that they are larger than Ni, is seen for all the SWNTs investigated here. It is also observed for metal carbon diatomic molecules, where Fe—C bond energy (−7.96 eV) is similar to Co—C (−7.23 eV), and these are larger than Ni—C (−5.91 eV), as calculated using VASP. Interestingly, this trend is not always observed when these metal atoms bond to the walls of CNTs or on top of graphene sheets (bonding with π bonds to make sp^3 bonds),[32,33] instead of at their ends or edges (bonding with sp^2 bonds keeping the graphitic structure intact).

As can be seen in Table I, the top sites are more stable than the middle sites for the M_5 ring and M_{13} cluster geometries. We suggest that this is due to sp^2-type directional bonding of the SWNT end atoms to the metal cluster atoms. Note that the top position coincides naturally with the continuation of the (5,0) SWNT, while for the single-atom model it is more favorable to passivate more carbon dangling bonds than to keep the sp^2 angles. This directional bonding has been observed previously for carbon atoms dissolved in metal clusters.[34] It is important to note that directional bonding cannot be described in analytic pairwise potential-energy models, and hence such models will not give correct minimum-energy structures.

As shown in Table II, similar results are obtained for the (10,0) SWNT, where the middle site is favored for the single atom but not for the M_{10} ring [a potential surface similar to

TABLE II. Adhesion energies (eV/atom) for Ni, Co, and Fe M_{55} cluster-(10,0) SWNT complex as obtained by VASP (see Method section). "Atom" and "ring" refer to approximate models for M_{55}. Results for completely relaxed ring structures and when the rings are constrained are shown. Energies when relaxing the isolated SWNTs (see Method section) are shown in parentheses.

		Adhesion energies (eV/atom)		
		Fe	Co	Ni
Atom	Top	−5.58	−5.33	−4.81
	Middle	−6.99	−6.69	−5.17
Ring (relaxed)	Top	−3.39 (−3.25)	−3.33 (−3.20)	−3.16 (−3.09)
	Middle	−2.78 (−2.66)	−2.87 (−2.76)	−2.96 (−2.86)
Ring (constrained)	Top	−3.65	−3.51	−3.17
	Middle	−3.12	−3.04	−2.94

that shown in Fig. 1 is obtained for the (10,0) SWNT]. The adhesion energies are similar to those of the (5,0) SWNT shown in Table I.

Figure 3 shows the adhesion energy of a single Ni atom bonded to different sites at the end of the (5,5) SWNT. Similar to Fig. 1, the atom is constrained to be in the cylindrical plane of the SWNT wall, and the nanotube is projected onto the plane of the page to show the metal atom positions with respect to the end carbon atoms. It is evident that there are two different minimum-energy sites: one denoted as "middle 1," where the atom lies between four SWNT end atoms, and the other as "middle 2," where the atom lies between two end atoms. The most stable structure, middle 1, is shown in Fig. 4(a). The adhesion energies of these structures, as well as for the unstable top site geometry, are listed in Table III for all three metals. Similar to the (5,0) and (10,0) zigzag SWNTs, Fe and Co have comparable adhesion energies that are larger than those for Ni.

As with the zigzag SWNTs, a very different potential surface is obtained for the ring compared to the single-atom model. The top site, shown in Fig. 4(b), is a minimum-energy site for the ring, and the adhesion energy at this site is similar to—or even slightly larger than—that at the middle site, shown in Fig. 4(c). When the ring is constrained to lie above the SWNT wall, the top site is consistently more stable than the middle site for all metals. The difference between the constrained and fully relaxed ring results is due to the fact that, in contrast to the zigzag SWNTs, the fully relaxed ring moves away from the SWNT wall and adopts a noncircular structure. The top views of the constrained and fully relaxed structures are shown in Figs. 4(e) and 4(f) for the top site and Figs. 4(g) and 4(h) for the middle site, respectively.

The large ring relaxation at the armchair end, which is not observed for the zigzag end, is due to the difference in chemistry between their open ends, which is also manifested in differences in the carbon-metal bond strengths. Comparing the energies in Tables I–III reveals that the carbon-metal adhesion strengths are far larger for the zigzag nanotubes than for the armchair nanotube. This is consistent with previous work,[13] where it was seen that zigzag SWNTs have larger edge energies than armchair SWNTs. The stronger carbon-metal bonds at the zigzag ends prevent restructuring of the

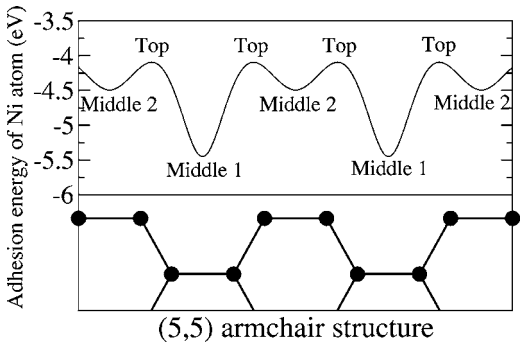

FIG. 3. Adhesion energy of a single Ni atom bonded to different sites at the end of a (5,5) SWNT.

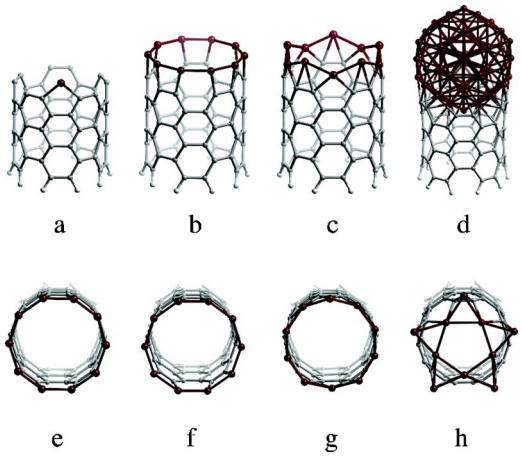

FIG. 4. (Color online) Structures of a (5,5) SWNT bonded to (a) a Ni atom, (b) the constrained Ni_{10} ring top site, (c) the constrained Ni_{10} ring middle site, and (d) a Ni_{55} cluster. Top views for the constrained and fully relaxed structures are shown in (e) and (f) for the Ni_{10} ring top site and in (g) and (h) for the Ni_{10} ring middle site.

TABLE III. Adhesion energies (eV/atom) for Ni, Co, and Fe M_{55} cluster-(5,5) SWNT complexes as obtained by VASP (see Method section). "Atom" and "ring" refer to approximate models for M_{55} (left column). Results for completely relaxed ring structures and when the rings are constrained are shown. Energies when relaxing the isolated SWNTs (see Method) are shown in parentheses.

		Adhesion energies (eV/atom)		
		Fe	Co	Ni
Atom	Top	−4.77	−4.56	−4.11
	Middle 1	−6.24	−5.94	−5.44
	Middle 2	−5.63	−5.20	−4.50
Ring relaxed	Top	−2.53 (−2.14)	−2.43 (−2.10)	−2.24 (−1.97)
	Middle	−2.55 (−2.08)	−2.59 (−2.16)	−2.26 (−1.89)
Ring constrained	Top	−2.61	−2.50	−2.23
	Middle	−2.24	−2.17	−2.04
Cluster	Middle	−1.82	−1.60	−1.51

M_5 and M_{10} rings in the (5,0) and (10,0) nanotube complexes, respectively.

As discussed above, the geometries and energies of the unconstrained ring structures are shown for completeness, but these are not directly relevant as approximative models for the full metal clusters M_{13} and M_{55}. Figure 4(d) shows the relaxed (5,5) SWNT-Ni_{55} structure, in which very little deformation of the metal cluster geometry can be seen. Due to computational limitations, only the middle two sites of the clusters have been calculated, and these are shown in Table II. In agreement with the results for the zigzag nanotubes, Fe and Co have similar adhesion energies and these are larger than for Ni.

We have shown that the SWNT-cluster adhesion needs to be sufficiently strong to prevent the SWNT end from closing (which will occur if the C—C bond strength is far larger than the carbon-metal bond strength).[18] Nanotube closure prevents further carbon addition to the SWNT end and hence stops nanotube growth. The SWNT-cluster adhesion strength may also affect the rate of SWNT growth as well as its chirality. For example, the results presented here show that Ni has weaker bonding to SWNTs than Fe and Co, and zigzag SWNTs have stronger bonding to all three metal clusters than armchair nanotubes. The effect that this has on nanotube growth and chiral control is being studied in our group.

Due to computational limitations, many DFT studies of large systems, including those presented here, focus on static, zero Kelvin structures. This differs from experimental SWNT growth conditions, where the high temperatures (typically 800 K) are expected to cause disordering of the metal cluster (e.g., bulk or surface melting of the cluster). This disorder may allow the metal cluster to adapt its shape to the structure of the SWNT end (instead of having the rigid crystalline structure studied here). The directional bonding between the SWNT end atoms and the cluster atoms discussed here may affect this cluster shape, and the effects of this bonding will change with increasing temperature (i.e., with the increasing importance of entropic effects). As discussed above, simple analytic force fields do not capture the directional bonding and molecular dynamics based on electronic structure forces (e.g., DFT) is required to study these effects. However, based on the results presented here, analytic force fields can provide a valid description of the trends in the cluster-SWNT adhesion energies.

CONCLUSIONS

Density-functional theory calculations have been used to study SWNT-metal cluster adhesion strengths for (5,0), (10,0), and (5,5) nanotubes bonded to Fe, Co, and Ni M_{13} and M_{55} clusters. Modeling these clusters by a single atom or as a ring of atoms yields the correct trend in adhesion energy, with Fe and Co being similar and larger than Ni. However, the single-atom model does not yield the correct minimum-energy structures and binding sites that are found for the full cluster SWNT complexes. In contrast, the metal ring model yields the correct binding sites, and we have shown that this is due to the fact that sp^2-type directional bonding of the SWNT end atoms to the metal governs bonding to the ring and cluster but not to the single atom.

These results, which are insensitive to the length of the SWNT used in the calculations, the computational software, density functional, and basis sets, are important contributions toward the understanding of SWNT growth, since all of the metals studied have SWNT-cluster adhesion energies that are sufficiently large to maintain open ends of growing SWNTs and hence enable continued growth. In addition, the difference in adhesion strengths between armchair and zigzag SWNTs may explain why certain nanotube chiralities are preferred in many chemical-vapor deposition experiments.[35]

ACKNOWLEDGMENTS

The authors are grateful for time allocated on Swedish National Supercomputing facilities and for financial support from the Swedish Research Council and the Swedish Foundation for Strategic Research (CARAMEL consortium), Science Foundation Ireland, and the Marie Curie early stage training network NANOCAGE (MEST-CT-2004-506854).

*Corresponding author. FAX: +46(0)31-7723496. Electronic address: Haiming.Duan@physics.gu.se

[1] S. Iijima and T. Ichihashi, Nature (London) **363**, 603 (1993).
[2] D. S. Bethune, C.-H. Kiang, M. S. de Vries, G. Gorman, R. Savoy, J. Vazquez, and R. Beyers, Nature (London) **363**, 605 (1993).
[3] M. P. Avantram and F. Leonard, Rep. Prog. Phys. **69**, 507 (2006).
[4] R. Krupke, F. Hennrich, H. v. Löhneysen, and M. M. Kappes, Science **301**, 344 (2003).
[5] M. Zheng, A. Jagota, E. D. Semke, B. A. Diner, R. S. McLean, S.

R. Lustig, R. E. Richardson, and N. G. Tassi, Nat. Mater. **2**, 338 (2003).
[6] D. Chattopadhyay, I. Galeska, and F. Papadimitrakopoulos, J. Am. Chem. Soc. **125**, 125 (2003).
[7] Z. Chen, X. Du, M.-H. Du, C. D. Rancken, H.-P. Cheng, and A. G. Rinzler, Nano Lett. **3**, 1245 (2003).
[8] M. S. Arnold, A. A. Green, J. F. Hulvat, S. I. Stupp, and M. C. Hersam, Nature Nanotechnol. **1**, 60 (2006).
[9] Y. Shibuta and S. Maruyama, Chem. Phys. Lett. **382**, 381 (2003).
[10] F. Ding, K. Bolton, and A. Rosén, J. Phys. Chem. B **108**, 17369 (2004).
[11] W.-Q. Deng, X. Xu, and W. A. Goddard III, Nano Lett. **4**, 2331 (2004).
[12] X. Fan, R. Buczko, A. A. Puretzky, D. B. Geohegan, J. Y. Howe, S. T. Pantelides, and S. J. Pennycook, Phys. Rev. Lett. **90**, 145501 (2003).
[13] Y. H. Lee, S. G. Kim, and D. Tománek, Phys. Rev. Lett. **78**, 2393 (1997).
[14] J. Gavillet, A. Loiseau, F. Ducastelle, S. Thair, P. Bernier, O. Stéphan, J. Thibault, and J.-C. Charlier, Carbon **40**, 1649 (2002).
[15] J.-Y. Raty, F. Gygi, and G. Galli, Phys. Rev. Lett. **95**, 096103 (2005).
[16] A. Moisala, A. G. Nasibulin, and E. I. Kauppinen, J. Phys.: Condens. Matt. **15**, S3011 (2003).
[17] A. Rochefort, D. R. Salahub, and P. Avouris, J. Phys. Chem. B **103**, 641 (1999).
[18] F. Ding, P. Larsson, J. Andreas Larsson, R. Ahuja, H. Duan, A. Rosén, and K. Bolton (unpublished).
[19] G. Kresse and J. Hafner, J. Phys.: Condens. Matt. **6**, 8245 (1994).
[20] G. Kresse and J. Hafner, Phys. Rev. B **47**, 558 (1993); **49**, 14251 (1994).
[21] G. Kresse and J. Furthmüller, Phys. Rev. B **54**, 11169 (1996).
[22] J. P. Perdew, J. A. Chevary, S. H. Vosko, K. A. Jackson, M. R. Pederson, D. J. Singh, and C. Fiolhais, Phys. Rev. B **46**, 6671 (1992).
[23] I. M. L. Billas, A. Chatelain, and W. A. de Heer, Science **265**, 1682 (1994).
[24] J. P. Bucher, D. C. Douglass, and L. A. Bloomfield, Phys. Rev. Lett. **66**, 3052 (1991).
[25] F. Ding, A. Rosén, and K. Bolton, Phys. Rev. B **70**, 075416 (2004).
[26] R. Ahlrichs, M. Bär, H. Häser, H. Horn, and C. Kölmer, Chem. Phys. Lett. **162**, 165 (1989).
[27] J. P. Perdew, K. Burke, and M. Ernzerhof, Phys. Rev. Lett. **77**, 3865 (1996).
[28] Y. Zhang, Y. Li, W. Kim, D. Wang, and H. Dai, Appl. Phys. A: Mater. Sci. Process. **A74**, 325 (2002).
[29] A. G. Nasibulin, P. V. Pikhitsa, H. Jiang, and E. I. Kauppinen, Carbon **43**, 2251 (2005).
[30] F. Ding, A. Rosén, and K. Bolton, J. Chem. Phys. **121**, 2775 (2004).
[31] K. Bolton, F. Ding, and A. Rosen, J. Nanosci. Nanotechnol. **6**, 1211 (2006).
[32] Y. Yagi, T. M. Briere, M. H. F. Sluiter, V. Kumar, A. A. Farajian, and Y. Kawazoe, Phys. Rev. B **69**, 075414 (2004).
[33] Y. L. Mao, X. H. Yan, and Y. Xiao, Nanotechnol. **16**, 3092 (2005).
[34] A. Arya and E. A. Carter, J. Chem. Phys. **118**, 8982 (2003).
[35] S. M. Bachilo, L. Balzano, J. E. Herrera, F. Pompeo, D. E. Resasco, and R. B. Weisman, J. Am. Chem. Soc. **125**, 11186 (2003).